Korean J. Chem. Eng., **23**(6), 1023-1027 (2006)

Adsorptive separation of rhenium and rhodium in nitric acid solution using a column packed with an extractant impregnated resin

Jei-Kwon Moon†, Chong-Hun Jung, Eil-Hee Lee and Byung-Chul Lee*

Korea Atomic Energy Research Institute, P.O. BOX 105 Yuseong, Daejeon 305-600, Korea
*Department of Chemical Engineering, Hannam University, Ojung, Daeduk, Daejeon 306-791, Korea
(*Received 17 May 2006 • accepted 30 June 2006*)

Abstract−An adsorptive separation of rhenium and rhodium was performed by using a jacketed glass column packed with an extractant impregnated resin (EIR). The EIR bed showed a successful separation of rhenium and rhodium with about 122 BV of a breakthrough volume. The breakthrough behavior in the column was modeled to assess the mass transfer resistances in the column. The model predicted the column dynamics for rhenium quite well by assuming a homogeneous diffusion in the particle phase. The effective diffusivities of rhenium were in the order of 10^{-7} cm^2/min. The EIR loaded beds could be eluted with a high purity of more than 99% by using a nitric acid solution.

Key words: Adsorptive Separation, Extractant Impregnated Resin, Technetium, Rhenium, Rhodium, Aliquat 336, Spent Fuel

INTRODUCTION

Tc-99 has a long half-life of 2.13×10^5 yr and reportedly exists with an amount of 0.77 kg per 1 ton of SNF. It exists in an aqueous solution as a pertechnetate ion, TcO_4^-, which is very mobile in soil, ground and surface waters. Technetium behaves as a nutrient analogue and possibly is concentrated by plants. The pertechnetate ion ingested by humans and animals is localized in the gastrointestinal tract and thyroid gland. For the bulk separation of technetium, normally a conventional extraction method has been applied more or less successfully [Asakura et al., 2004; Funasaka et al., 2000]. However, because of a high radio toxicity of technetium even when its concentration is very low, new materials and methods other than conventional liquid-liquid extraction are required for application to a low concentration solution. Adsorptive separation by using an extractant impregnated resin (EIR) has been reviewed as a promising method to obtain a high selectivity for both low and high concentration solutions, since it combines the characteristic advantages of ion exchange and extraction. Overview on the concept and the characteristic advantages of the EIR are described well in some papers [Cortina and Warshawsky, 1997; Kaby et al., 2003]. Some research results on the separation of technetium from environmental samples by using composite ion exchangers have also been reported [Bartosova et al., 2004; Uchida and Tagami, 1997]. They used a TEVA-Spec resin where Aliquat 336 is incorporated with a silica gel support. In our previous work [Moon et al., 2006], we also successfully performed research on the preparation of an EIR for the removal of rhenium, which is a chemical analogue of technetium. We evaluated the equilibrium parameters such as the maximum adsorption capacities and the equilibrium constants based on the Langmuir model, and we also estimated the diffusivities for a batch-wise kinetic system by assuming a homogeneous diffusion in the solid phase.

†To whom correspondence should be addressed.
E-mail: njkmoon@kaeri.re.kr

In this study, as an extension of our previous research, we carried out an adsorptive separation of rhenium and rhodium by using a jacketed glass column packed with the EIR (XAD-4 Resin Impregnated with Aliquat 336). Breakthrough behavior for the single and mixed component solutions was investigated. The breakthrough curves were modeled mathematically to understand the mass transfer resistances in the column.

MATHEMATICAL MODELING

A mathematical model was developed to describe the behavior of the packed beds for an adsorption. The model is illustrated in Fig. 1.

It is assumed that the fluid phase containing the components to be adsorbed enters the bed at the bottom and exits from the top of the column. The model was developed by assuming the mass trans-

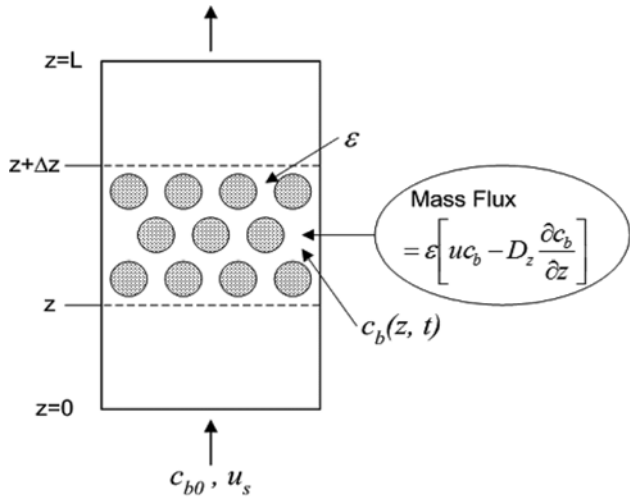

Fig. 1. Schematic representation of a packed-bed adsorption column model.

fer effects due to an intraparticle diffusion, liquid film mass transfer, and axial dispersion. It was assumed that the axial dispersion is negligible for the long-bed column and concentration gradients exist only in the axial direction. In this work, mass transfer by axial dispersion was neglected. The particles in the column were considered to be homogeneous, and thus a homogeneous diffusion model was applied to describe intraparticle diffusion. Therefore, the model incorporates the mathematical descriptions of the following processes; (1) mass transfer resistance in the liquid film surrounding the adsorbent particle, (2) local equilibrium adjacent to the exterior surface of the adsorbent, and (3) diffusion resistance within the particle. In Fig. 1, $c_b(z, t)$ is the cation concentration in the bulk fluid at a certain column height and time, $c_s(z, t)$ is the cation concentration in the liquid phase at the particle surface at the same position, and $q(z, r, t)$ is the cation concentration inside the homogeneous solid phase. At the particle surface, c_s is in equilibrium with q. It is assumed that the system is isothermal and the ion exchange rate is much faster than the diffusion rate. Therefore, the ion exchange rate does not affect the kinetics of the system.

The overall mass balance in a long packed-bed column with no axial dispersion leads to the following relationship for mass transfer in the axial direction:

$$-u\frac{\partial c_b}{\partial z}=\frac{\partial c_b}{\partial t}+\frac{\rho(1-\varepsilon)}{\varepsilon}\frac{\partial \bar{q}}{\partial t} \tag{1}$$

where u is the interstitial velocity ($u=u_s/\varepsilon$), u_s is the flow rate of the feed solution into the column inlet, ε is the void fraction in the column, ρ is the particle density, and $\bar{q}$ is the average concentration in the solid phase.

The diffusion in the solid phase is assumed to follow Fick's law. The unsteady-state diffusion in a homogeneous solid sphere can be described by the following partial differential equation:

$$\frac{\partial q}{\partial t}=\frac{1}{r^2}\frac{\partial}{\partial r}\left(r^2 D_p\frac{\partial q}{\partial r}\right) \tag{2}$$

where D_p is the solid phase diffusivity for an ion. If D_p is concentration-dependent, it can be represented by Darken's law:

$$D_p=D_p^0\frac{d\ln c}{d\ln q}=D_p^0 H(q) \tag{3}$$

where D_p^0 is the corrected diffusivity, independent of the concentration. Substituting Eq. (3) into Eq. (2) gives

$$\frac{\partial q}{\partial t}=D_p^0\left[H(q)\frac{1}{r^2}\frac{\partial}{\partial r}\left(r^2\frac{\partial q}{\partial r}\right)+\frac{\partial H(q)}{\partial r}\frac{\partial q}{\partial r}\right] \tag{4}$$

At the particle surface, where $r=R_p$, equilibrium exists between the liquid phase concentration (c_s) and the solid phase concentration (q). In this work we used the Langmuir isotherm:

$$q=\frac{ac_s}{1+bc_s} \qquad \text{at } r=R_p \tag{5}$$

Thus, Darken's law in Eq. (3) is given by the following equation.

$$H(q)=\frac{a}{a-bq} \tag{6}$$

A material balance at the particle surface leads to the following boundary condition:

$$\frac{\partial \bar{q}}{\partial t}=\frac{3}{R_p^3}\int_0^{R_p}\frac{\partial q}{\partial t}r^2\,dr=\frac{3k_f}{\rho R_p}(c_b-c_s) \qquad \text{at } r=R_p \tag{7}$$

where k_f is the mass transfer coefficient in the liquid film around the particle. Eq. (7) can be modified by substituting Eq. (2) into the integral in Eq. (7).

$$\left[H(q)\frac{\partial q}{\partial r}\right]_{r=R_p}=\frac{k_f}{\rho D_c^0}(c_b-c_s) \qquad \text{at } r=R_p \tag{8}$$

Thus,

$$c_s=c_b-\frac{\rho R_p}{Bi}\left[H(q)\frac{\partial q}{\partial r}\right]_{r=R_p} \qquad \text{at } r=R_p \tag{9}$$

where Bi is the non-dimensional Biot number defined as:

$$Bi=\frac{k_f R_p}{D_c^0/R_p^2} \tag{10}$$

The Biot number measures the relative resistance from the liquid film surrounding the particle to the internal diffusion resistance.

Substituting Eq. (7) into Eq. (1) gives the following overall mass balance equation:

$$-u\frac{\partial c_b}{\partial z}=\frac{\partial c_b}{\partial t}+\frac{3(1-\varepsilon)k_f}{\varepsilon R_p}(c_b-c_s) \tag{11}$$

Finally, the boundary condition in the axial direction is:

$$c_b=c_{b0} \qquad \text{at } z=0 \tag{12}$$

And the initial conditions are:

$$c_b=c_s=q=0 \qquad \text{at } t=0\ (z>0) \tag{13}$$

The above equations can be rewritten in a dimensionless form by introducing the following dimensionless variables:

$$C_b=\frac{c_b}{c_{b0}},\quad C_s=\frac{c_s}{c_{b0}},\quad Q=\frac{q}{q_0},\quad \lambda=\frac{r}{R_p},\quad \xi=\frac{z}{L},\quad \tau=\frac{ut}{L} \tag{14}$$

where q_0 is in equilibrium with c_{b0}. The overall mass balance, Eq. (11) becomes

$$\frac{\partial C_b}{\partial \tau}=-\frac{\partial C_b}{\partial \xi}-\frac{3(1-\varepsilon)St}{\varepsilon}(C_b-C_s) \tag{15}$$

where St is the Stanton number defined as:

$$St=\frac{k_f R_p}{u/L} \tag{16}$$

With the dimensionless variables, Eqs. (4) and (9) become

$$\frac{\partial Q}{\partial \tau}=\frac{D_p^0 L}{R_p^2 u}\left[H(Q)\frac{1}{\lambda^2}\frac{\partial}{\partial \lambda}\left(\lambda^2\frac{\partial Q}{\partial \lambda}\right)+\frac{\partial H(Q)}{\partial \lambda}\frac{\partial Q}{\partial \lambda}\right] \tag{17}$$

$$C_s=C_b-\frac{\rho q_0}{c_{b0}Bi}\left[H(Q)\frac{\partial Q}{\partial \lambda}\right]_{\lambda=1} \qquad \text{at } \lambda=1 \tag{18}$$

For the Langmuir isotherm,

$$Q=\frac{ac_{b0}C_s}{q_0(1+bc_{b0}C_s)} \qquad \text{at } \lambda=1 \tag{19}$$

$$H(Q)=\frac{a}{a-bq_0Q}=1+bc_{b0}C_s \tag{20}$$

The boundary and initial conditions can be expressed as:

$$C_b=1 \qquad \text{at } \xi=0 \tag{21}$$

$$C_b=C_s=Q=0 \qquad \text{at } \tau=0\ (\xi>0) \tag{22}$$

These equations constitute a set of partial differential equations (PDEs) which should be solved by a numerical method. In this work, we converted the PDEs into ordinary differential equations (ODEs) by using the orthogonal collocation method [Villadsen and Michelsen, 1978]. Then a set of ODEs was solved by utilizing the IMSL/Math subroutine IVPAG, which is based on the Gear's stiff integration algorithm.

The film mass transfer coefficient, k_f, used for an evaluation of the effective diffusivity was estimated by using a correlation developed for packed beds by Williamson et al. as follows:

$$Sh=2.4\varepsilon Re^{0.34}Sc^{0.42} \tag{23}$$

The average absolute deviation percent of a determination (AAD%) was calculated by using an equation defined as

$$AAD(\%)=\frac{1}{n}\sum_{i=1}^{n}\frac{|C_{b,i}^{calc}-C_{b,i}^{exp}|}{C_{b,i}^{exp}}\times 100 \tag{24}$$

where,

$C_{b,i}^{calc}$: dimensionless bulk phase concentration calculated by the model

$C_{b,i}^{exp}$: experimental value of the dimensionless bulk phase concentration

n : number of data points

EXPERIMENTAL

A jacketed glass column (∅11×L150, Bed Volume=14.25 mL) was used for the column experiments. The column was kept constant at 25 °C in a water jacket. About 82 grams of an EIR was washed with distilled water and filled into the column. The test solutions of rhenium were prepared by dissolving Re_2O_3 (Aldrich) in a 0.5 M nitric acid solution. $Rh(NO_3)_3$ (Aldrich) was used for the rhodium sources. The effect of the flow rate on the breakthrough behavior of the column was investigated with a rhenium solution of 100 ppm in the range of 4.3-7.5 mL/min (4.5-7.9 cm/min). The mixed solutions of the rhenium and rhodium ions were passed through the column and then the samples were collected with a fractional collector. The concentrations of the effluent samples were measured by using an AAS (GBC Co., Model 906). Elution behavior of the rhenium and rhodium from the loaded beds was investigated with a HNO_3 solution.

RESULTS AND DISCUSSION

1. Effect of Flow Rate on the Breakthrough Behavior

Fig. 2 shows the breakthrough behavior of the rhenium ion depending on the flow rate within the range between 4.3 mL/min and 7.5 mL/min. At a flow rate of 4.3 mL/min, the breakthrough curves show a long tail with a breakthrough volume less than 100 BV for a 1% breakthrough. As the flow rate increases from 4.3 to 5.2 mL/min, the breakthrough volume increases from about 90 BV to about 120 BV and the breakthrough curve becomes steeper. The same trend is also observed at different flow rates up to 6.2 mL/min to obtain about 130 BV of a 1% breakthrough volume. However, a further increase of the flow rate results in a drastic decrease of the breakthrough volume. Therefore, the flow rate of 6.2 mL/min (6.5 cm/min) was used in the following column experiments.

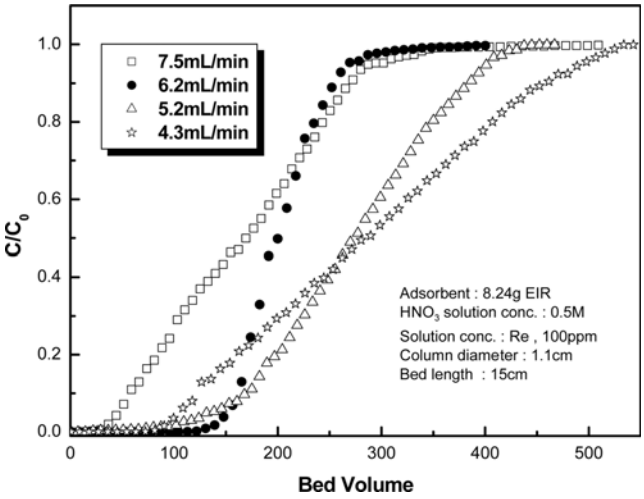

Fig. 2. Effect of flow rate on the breakthrough behavior of rhenium ion in the EIR column.

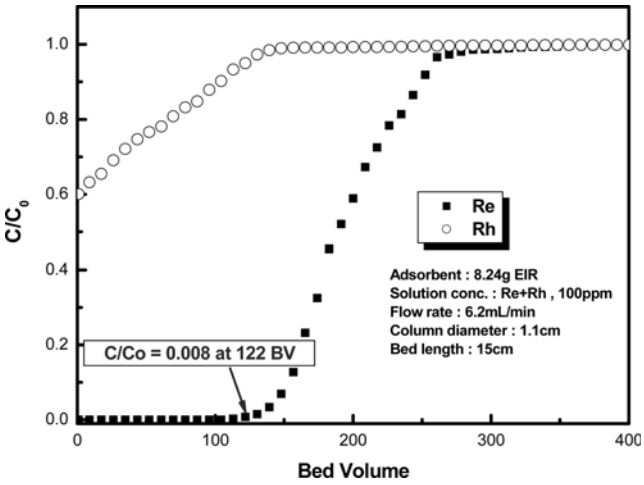

Fig. 3. Breakthrough curves for the mixed solution of rhenium and rhodium ions in the EIR column.

2. Breakthrough behavior for the Mixed Solutions

Breakthrough curves for the mixed solutions of the rhenium and rhodium ions are shown in Fig. 3.

The solution concentration is 100 ppm. The breakthrough volume is about 122 BV for rhenium when 0.8% of an initial concentration is considered as a breakthrough point. Within this volume, very pure rhodium of more than 99% is recovered. The breakthrough curve reaches its saturation point at about 270 BV and then the loading capacity for rhenium becomes about 1.30 meq/g. On the other hand, the breakthrough curve of rhodium starts at about 0.6 of an initial concentration and reaches its saturation point at a bed volume of less than 150 with a loading capacity of about 0.09 meq/g. As we described in our previous research [Moon et al., 2006], it is due to the fact that the rhodium ion in a nitric acid solution exists mainly in the form of oligomers with a positive charge which is hard to be adsorbed onto anion exchangers.

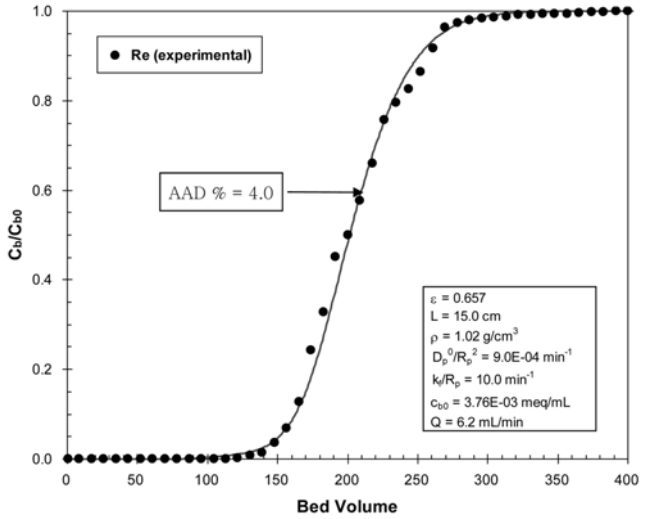

Fig. 4. Modeling example for the breakthrough cure of the rhenium ion in the EIR column.

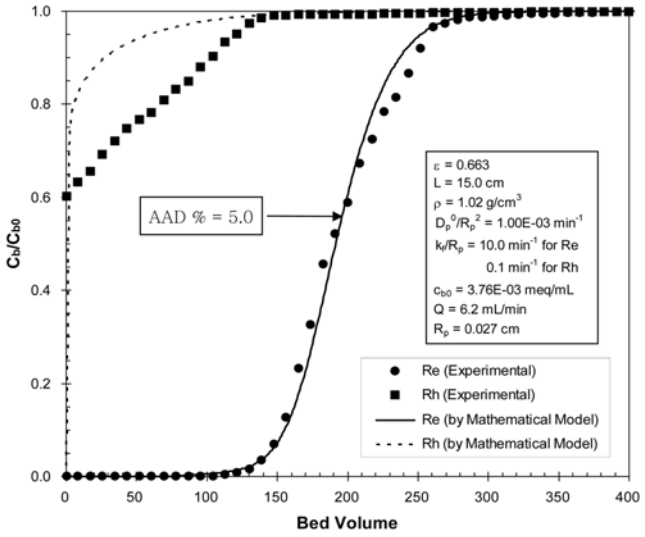

Fig. 5. Modeling examples for the breakthrough cures of the mixed solution of rhenium and rhodium ions in the EIR column.

3. Modeling of the Breakthrough Curves

The breakthrough curves for the rhenium and rhodium ions were modeled to evaluate the effective diffusivities for the EIR column. Modeling examples for the single and the two component systems are shown in Figs. 4 and 5, respectively. For the single component system shown in Fig. 4, the model predicts the experimental data quite well. The diffusion time constant for rhenium obtained by the modeling is 9.0×10^{-4} min^{-1}. Since the particle radius is 0.027 cm, the effective diffusivity for rhenium is 6.6×10^{-7} cm^2/min. The modeling results for the two component system, as given in Fig. 5, also show a successful simulation for the breakthrough curve of rhenium.

The diffusion time constant is almost the same as that for the single component system. However, in the case of rhodium, the model does not predict the experimental data. This might be caused by inaccurate estimation of the equilibrium parameters due to unfavorable adsorption of rhodium [Moon et al., 2006]. The effective diffusivities obtained for an adsorption of rhenium and rhodium with the EIR column are rather new ones, so they could not be compared with other results directly. However, they are comparable with our previous results obtained from a kinetic study in a batch reactor [Moon et al., 2006]. The average absolute deviation percentage (AAD%) between the experimental and calculated values ranges from 4.0 to 5.0 for the simulation of the breakthrough curves for rhenium, which are well within the limits of accuracy for the diffusivities reported in the literature. Typical deviations for the intraparticle diffusivities are reportedly ±3-8% [Robinson et al., 1994].

4. Elution Behavior

For desorbing rhenium from the loaded bed, NH_4Cl, HCl and HNO_3 were tested as the candidates for the desorbing solutions. The tests were performed in a batch reactor and the concentrations of the tested solutions were varied in the range between 0.5 M and 5 M. Among them, the 5 M HNO_3 solutions showed the best desorbing performance. It is natural that the desorbing performance is proportional to the solution concentration. However, by considering the difference in the separation efficiency between the rhe-

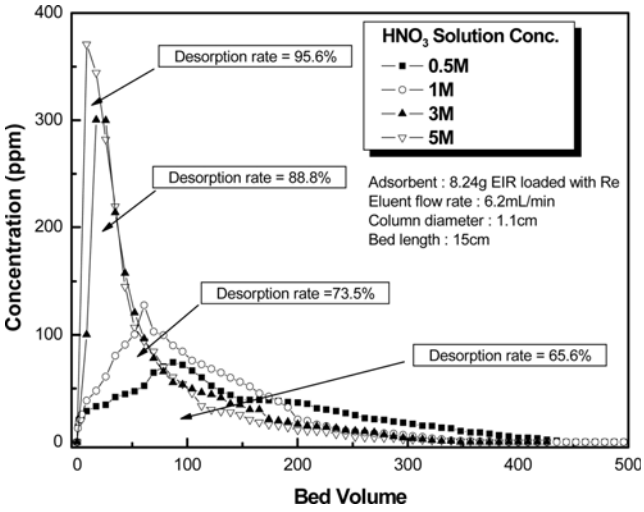

Fig. 6. Effect of HNO_3 concentration on the desorption of rhenium from the loaded bed.

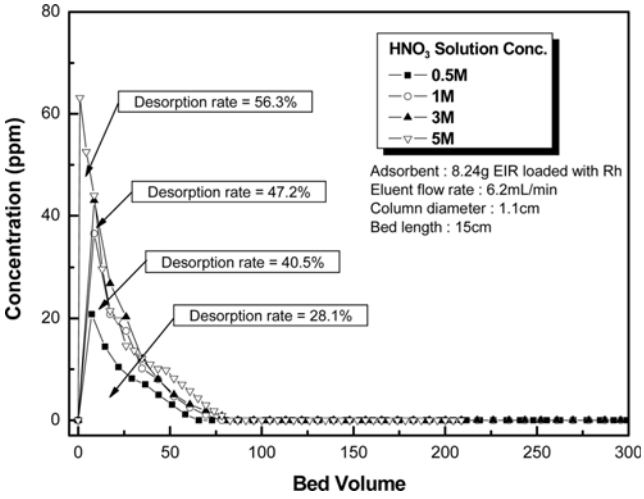

Fig. 7. Effect of HNO_3 concentration on the desorption of rhodium from the loaded EIR bed.

nium and rhodium ions, a fractional desorption is considered. In order to confirm this fact, the desorption behavior of rhenium and rhodium from the loaded beds was investigated with various nitric acid concentrations as shown in Figs. 6-7. In the case of the rhenium ion, the elution curve becomes wider as the nitric acid concentration becomes lower. However, in the case of the rhodium ion, the shape of the elution curves does not change, although the desorption capacity is reduced. This means that rhenium is more sensitive to the concentration of a desorbing solution. Since a higher concentration of a desorbing solution could bring about a simultaneous desorption of both components, the concentration of the desorbing solution was lowered to 0.5 M in the first cycle and then increased to 1 M in the second cycle as shown in Fig. 8. It was shown that about 65% of rhenium was desorbed in the first desorption step after about a 470 BV elution with a 0.5 M HNO_3 solution, and 33% in the second step after about a 350 BV elution with a 1 M HNO_3 solution.

The relation between the purity and recovery for the rhenium is summarized in Table 1.

As shown in the table, the total recovery for rhenium is about 98% and the purity is 97.5%. The recovery, however, can be controlled by fractionally collecting the elution volume depending on the desired purity. Thus, if the recovery is reduced to 94.6%, the purity becomes more than 99%. These results, although they are the results for a chemical analogue of Tc, show the possibility for a recovery of radioactive technetium from a nuclear stream. On the other hand, rhodium, due to its complex chemical forms in a nitric acid solution, would require other methods for a selective separation.

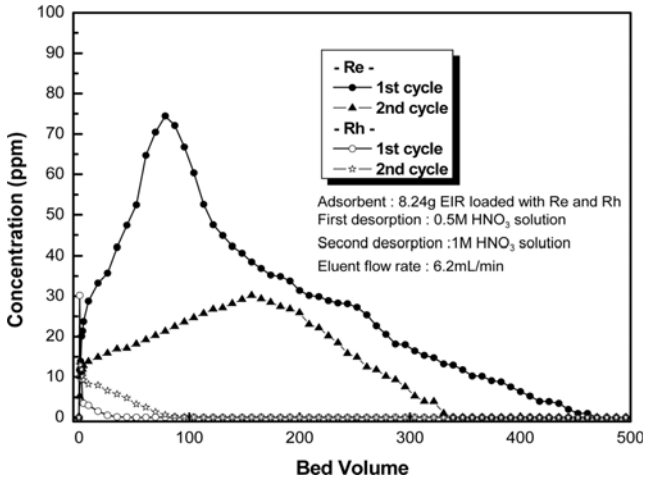

Fig. 8. Cycling elution of the rhenium and rhodium ions from the loaded EIR bed.

Table 1. Relation between recovery and purity of rhenium for the desorption steps

1st step (desorption with 0.5 M nitric acid)		2nd step (desorption with 1 M nitric acid)		Total	
Recovery (%)	Purity (%)	Recovery (%)	Purity (%)	Recovery (%)	Purity (%)
64.5	99.4	33.0	95.2	97.5	98
62.3	99.9	30.1	98.9	94.6	99.2
60.9	99.9	27.0	99.9	91.5	99.5
51.3	99.9	17.9	100.0	89.3	99.9

CONCLUSION

Adsorptive separation of rhenium and rhodium was performed by using a glass column packed with an EIR. The optimum flow rate determined for a maximum utilization of the bed was 6.2 mL/min. The EIR bed showed better adsorption performance for rhenium over rhodium with a breakthrough volume of 122 BV for rhenium when 0.8% of an initial concentration was considered as a breakthrough point. The breakthrough curve reached its saturation point at about 300 BV, and at this point the loading capacity for rhenium was about 1.30 meq/g. The breakthrough behavior in the column was modeled to assess the mass transfer resistances in the column. The model predicted the column dynamics for rhenium quite well and the effective diffusivities of rhenium were 10^{-7} cm^2/min in order of magnitude. The loaded beds were eluted effectively with nitric acid with a high purity of more than 99%.

ACKNOWLEDGMENTS

This work has been carried out under the Nuclear R&D program by MOST.

REFERENCES

Asakura, T., Hotoku, S., Ban, Y., Kim, S. Y., Mineo, H. and Morita, Y., *Research on PARC for future reprocessing*, ATLANTE 2004, Nimes, 012-04 (2004).

Bartosova, A., Rajec, P. and Reich, M., "Preparation and characterization of an extraction chromatography column for technetium separation based on Aliquat 336 and silica gel support," *J. Radioanalytical Nuclear Chem.*, **261**, 119 (2004).

Cortina, J. L. and Warshawsky, A., "Developments in solid-liquid extraction by solvent-impregnated resins," *Ion Exchange and Solvent Extraction*, **13**, 195 (1997).

Funasaka, H., Sano, Y., Nomura, K., Koma, Y. and Koyama, T., *Current status of research and development on partitioning of long-lived radionuclides in JNC*, ATLANTE 2000, 02-01 (2000).

Kabay, N., Arda, M., Saha, B. and Street, M., "Removal of Cr(VI) by solvent impregnated resins (SIR) containing Aliquat 336," *Reactive & Functional Polymers*, **54**, 103 (2003).

Moon, J. K., Han, Y. J., Jung, C. H., Lee, E. H. and Lee, B. C., "Adsorption of rhenium and rhodium in nitric acid solution by amberlite XAD-4 impregnated with Aliquat 336," *Korean J. Chem. Eng.*, **23**, 303 (2006).

Robinson, S. M., Arnold, W. D. and Byers, C. H., "Mass-transfer mechanisms for zeolite ion exchange in wastewater treatment," *AIChE J.*, **40**, 2045 (1994).

Uchida, S. and Tagami, K., "Separation and concentration of technetium using a Tc-selective extraction chromatographic resin," *J. Radioanalytical Nuclear Chem.*, **221**, 35 (1997).

Villadsen, J. and Michelsen, M. L., *Solution of differential equation models by polynomial approximation*, Prentice-Hall, Englewood Cliffs, NJ (1978).